Journal of Materials Chemistry B

Accepted Manuscript

ROYAL SOCIETY OF CHEMISTRY

www.rsc.org/materialsB

Journal Name

RSCPublishing

ARTICLE

In vivo assessment of grafted cortical neural progenitor cells and host response to functionalized self-assembling peptide hydrogels and the implications for tissue repair.

Cite this: DOI: 10.1039/xoxxoooooox

Received ooth January 2012,
Accepted ooth January 2012

DOI: 10.1039/xoxxoooooox

www.rsc.org/

A. L. Rodriguez[a], T. Y. Wang[b], K. F. Bruggeman[a], C. C. Horgan[a], R. Li[c], R. J. Williams[c, d], C. L. Parish[b]* and D. R. Nisbet[a]*

Tissue specific scaffolds formed from minimalist N-fluorenylmethyloxycarbonyl self-assembling peptides (Fmoc-SAPs) have emerged as promising biomaterials due to their ease of synthesis and capacity to self-assemble via simple, non-covalent interactions into complex nanofibrous hydrogels. However, concerns remain over their biocompatibility and cytotoxicity for *in vivo* applications. Here, we demonstrate that these Fmoc-SAPs are biocompatible *in vivo* and well suited as a delivery vehicle for cell transplantation. In order to determine the effect of tissue specific parameters, we designed three Fmoc-SAPs containing varying bioactive peptide sequences derived from extracellular matrix proteins, laminin and fibronectin. Fmoc-SAPs delivering cortical neural progenitor cells into the mouse brain display a limited foreign body response, effective functionalization and low cytotoxicity for at least 28 days. These results highlight the suitability of Fmoc-SAPs for improved neural tissue repair through the support of grafted cells and adjacent host parenchyma. Overall, we illustrate that Fmoc-SAPs are easily engineered materials for use as a tool in cell transplantation, where biocompatibility is key to promoting cell survival, enhancing the graft-host interface and attenuation of the inflammatory response for improved tissue repair outcomes.

Introduction

Central nervous system (CNS) repair presents a significant challenge, given the limited regenerative capacity of neural tissue. Currently, following insult to the CNS, treatments are limited to pharmacotherapy or rehabilitation with the aim of slowing disease progression and reducing secondary damage; thereby reducing symptom severity, without actually repairing the induced damage.[1] Cell replacement therapy offers an attractive alternative, whereby cells are implanted into the site of injury in order to regenerate and repair damaged neural tissue, providing symptomatic relief to patients.[2]

Early transplantation trials have identified additional mechanisms for repair, where grafted cells have been shown to be neuroprotective by providing trophic support to the surrounding area, attenuating the inflammatory response, promoting endogenous stem cell neurogenesis and enhancing angiogenesis.[3-5] Biomaterials have emerged as potential adjuncts for such tissue repair by delivering a morphological and biochemical extracellular matrix (ECM) mimic that can support transplanted cells at an injury site, lessening the impact of further degeneration to surrounding tissue and ultimately repairing the induced damage. As such, there is a need for biocompatible, functionalized materials into which cells can be embedded as a vector for transplantation, and once implanted *in vivo*, can attenuate the inflammatory response and allow the transplanted cells to infiltrate the host tissue by creating a permissive graft-host interface.

With this in mind, an ideal biomaterial for cell transplantation would improve recovery by creating a favorable milieu for exogenous and endogenous cells.[6] This would involve controlling the inflammatory response associated with the primary insult and ensuing transplantation surgery, which includes local astrocyte proliferation that can ultimately result in distortion of the brain parenchyma and scarring.[7] We have previously demonstrated the potential of electrospun scaffolds to modulate the inflammatory response of the brain with limited immunogenic reactivity.[8] However, while these

scaffolds were shown to mimic the ECM morphology and control the inflammatory response, their geometric constraints and fixed form does not allow them to readily interface with cells at the edge of a lesion site, making them less attractive for cell transplantation within the brain.[8, 9]

Nature utilizes supramolecular interactions to drive the self-organization of biological macromolecules such as peptides and proteins of the ECM.[10] These principles can be used to design synthetic peptides that can self-assemble into larger, complex structures, reminiscent of those found within living systems, providing a platform for the development of regenerative therapies.[11] Peptide based materials can be rationally designed to include features that emulate the ECM in an effort to reproduce the nanofibrous network of proteins, as well as provide control over the introduction of biochemical cues, such as the release of growth factors and presentation of integrin binding domains.[11, 12]

A number of hydrogels formed from fibrous self-assembling peptides (SAPs) have been developed for various *in vitro* and *in vivo* applications.[11] Significant progress has been made by utilizing long, highly structured peptides, such as the commercially available RADA16, or peptide amphiphiles.[13, 14] However, due to their lengthy amino acid chains, these peptides require a large number of steps to synthesize and purify - increasing cost and complexity whilst reducing yield. Consequently, considerable interest has surrounded the design of minimalist peptide sequences (1 - 10 residues), as these simple molecules retain the ability to self-assemble, whilst allowing the incorporation of bioactive sequences. Additionally, they enable the effect of individual amino acid modifications to be investigated, enabling fine control over the structure, assembly conditions and triggering mechanisms of the resulting macroscale hydrogel.[12, 15, 16]

A promising class of these materials is based on the assembly of SAPs capped at the N–terminal with fluorenylmethyloxycarbonyl (Fmoc). Fmoc-SAPs have been shown to self-assemble into nanofibers via non-covalent π-β interactions with the peptide sequence presented on the external surface of the fibrils at high density.[17, 18] These fibrils then intertwine to form an entangled matrix hydrogel that has morphological and mechanical similarities to many types of ECM.[17, 19] Fmoc-SAP hydrogels that morphologically emulate the native ECM are of particular interest due to their potential to effectively fill a void at the site of neural damage, readily interface with cells at the edge of the lesion site, attenuate the inflammatory response post implantation and structurally support the surrounding neural tissue.

Though the material characteristics and underlying self-assembly mechanism of Fmoc-SAPs have been thoroughly studied, investigation of their biological properties and how cells respond to their physical and biochemical stimuli has been limited - usually focusing on *in vitro* cell culture, incorporating the fibronectin based sequence, arginine-glycine-aspartate (RGD).[15, 17, 19-23] Additionally, research has typically focused on short di- and tripeptides, as the individual amino acid contributions in longer peptide sequences tend to inhibit spontaneous self-assembly under physiological conditions.[12] We have recently published novel approaches that allow core amino acid sequences of up to five residues in length to be embedded into the peptide backbone by the rational design of additional flanking residues; either through adjustment of pKa or addition of aromatic/hydrophobic residues.[12, 24] Using these methods, we have designed Fmoc-SAPs that contain peptide sequences based on the common ECM brain protein laminin: isoleucine-lysine-valine-alanine-valine (IKVAV) and tyrosine-isoleucine-glycine-serine-arginine (YIGSR).

We have previously demonstrated the functionality of the embedded peptide sequence in Fmoc-SAPs *in vitro*, compared to a morphologically and chemically similar system made from a scrambled control sequence.[24] Here, we examine the effect of these Fmoc-SAPs on primary cortical neural progenitor cells *in vivo*. In order to ascertain the effectiveness of these laminin peptide sequences *in vivo*, we also included an RGD containing Fmoc-SAP as a control, as fibronectin is known to promote cell adhesion and is not observed in significant amounts in the brain, allowing us to determine the tissue specificity of the Fmoc-SAPs.[25] Importantly, for the material to be effective, it must be well tolerated by both the host and implanted cells, and elicit a limited inflammatory response with limited or no formation of a glial scar. Therefore, the inflammatory response to these developed Fmoc-SAPs, as well as survival, migration and integration of the transplanted cortical neural progenitor cells were investigated in the intact brain. These results allow us to ascertain which peptide sequence has the most beneficial effect on endogenous and grafted cells *in vivo* for future application in the injured CNS.

Materials and methods

Solid phase peptide synthesis/Mass spectrometry. Fmoc-SAPs were made using solid phase peptide synthesis (SPPS) in a custom rotating glass reactor vessel at a 0.4 mmol scale. Fmoc protected amino acids, Hydroxybenzotriazole (HOBt), O-Benzotriazole-N,N,N',N'-tetramethyl-uronium-hexafluoro-phosphate (HBTU) and Wang based resins were purchased from GL Biochem (China). All other chemicals were purchased from Sigma-Aldrich. Dimethylformamide (DMF) was dried for a minimum of 2 hours prior to use with 4 Å molecular sieves.

Peptide synthesis was achieved by the stepwise deprotection of the N-terminal Fmoc group of the resin anchored amino acid using a solution of 20% piperidine in DMF, followed by a coupling step using a solution of the next Fmoc-amino acid in HOBt, HBTU and N,N-diisopropylethylamine (DIPEA) in DMF. This process of deprotection and coupling of amino acids was repeated until the desired peptide was synthesised. The final Fmoc group was not removed. Deprotection and coupling of amino acids was verified using a Kaiser test for the detection of free amines. Once SPPS of the desired sequence was complete, the Fmoc protected peptide and resin was washed with ethanol and left to dry under constant vacuum for 2 days. A cleavage solution of trifluororoacetic acid (TFA), 2.5% distilled water and 2.5% triethylsilane (TES) was prepared. The resin was left to stand in the solution for 2 hours. Following cleavage, the peptide solution was filtered through glass wool. Excess TFA was then evaporated using nitrogen until approximately 5 mL of peptide solution was left. The peptide was then precipitated, followed by 5 washes in cold ether before being collected and allowed to dry under constant vacuum for 2 days. The peptide was then ground into a fine powder before being placed under constant vacuum for a further 7 days. Mass spectrometry was performed to verify synthesis of the desired peptide.

Fmoc-SAP gel preparation. Fmoc-SAPs were prepared at 20 mg/mL. Approximately 10 mg of the peptide was initially dissolved in 100 µL deionized water with 50 µL of 0.5 M sodium hydroxide (NaOH). The pH of the peptide solution was then slowly reduced by the dropwise addition of 0.1 M hydrochloric acid (HCl) until the pH of the media was achieved (typically 100 - 150 µL). The solution was continually vortexed throughout this process. Once a gel was formed at appropriate pH, Hank's buffered saline solution (HBSS) (Gibco) was added to make the gel up to 20 mg/mL. The pH of the Fmoc-SAPs was measured using a microprobe pH meter.

Fourier transform infrared spectroscopy. Fourier transform infrared spectroscopy (FTIR) was performed using an Alpha Platinum Attenuated Total Reflectance FTIR (Bruker Optics). 30 μL of Fmoc-SAP was placed on the single reflection diamond. The pressure applicator was used to spread the Fmoc-SAP over the crystal. Absorbance scans were taken at 0 minutes and 5 minutes, with 5 minutes showing higher resolution.

Circular dichroism spectroscopy. Circular dichroism (CD) was completed using a Chirascan CD Spectrometer (Applied Photophysics Limited). Fmoc-SAP solutions were prepared at 1 part in 200 with deionized water. A baseline scan for deionized water was completed and subtracted from the obtained peptide CD scans. The Fmoc-SAP solution was scanned from 350 to 170 nm at a step size of 1 and 1 nm bandwidth.

Rheology. Viscoelastic properties of the formed Fmoc-SAPs were assessed using a Kinexus Pro+ Rheometer (Malvern). A 20 mm smooth flat plate with a solvent trap was used. The Fmoc-SAP sample was placed on the rheometer plate at a gap size of 0.2 mm. Oscillatory strain of 0.1% strain was used with a frequency sweep of 0.1 – 100 Hz.

Atomic force microscopy. Atomic force microscopy (AFM) images of the Fmoc-SAPs were obtained using a Multimolde 8 (Bruker BioSciences Corporation, USA). For sample preparation, 15 μL Fmoc-SAP was applied on highly ordered pyrolytic graphite (HOPG) substrates (SPI, USA). The tips used were scanasyst-air probes with silicon tip on nitride lever (Bruker BioSciences Corporation, USA). The AFM was operated in peak force QNM. Calibration of deflection sensitivity, spring constant and tip radius of probes was done before sample imaging. Scan size was at 10 μm.

Transmission electron microscopy. Transmission electron microscopy (TEM) was performed on a HITACHI HA7100 TEM with LaB6 filament at 100 kV. Negative stains were performed to image the Fmoc-SAP samples. Formvar coated copper grids were glow discharged for 30 seconds at 15 mA. A drop of the Fmoc-SAP sample was placed on the grid for 30 seconds, after which any excess was blotted off using filter paper. The grid was then washed with a drop of water, any excess water blotted off and the wash repeated. The grid was then briefly placed in a drop of 0.75% uranyl formate, blotted off and placed in a second drop of uranyl formate for 20 seconds. Any excess stain solution was blotted off and the grid was allowed to dry overnight before imaging in the TEM.

Preparation of primary cortical cells for transplantation. All procedures were conducted in accordance with the Australian National Health and Medical Research Council's published Code of Practice for the Use of Animals in Research and experiments were approved by the Florey Institute of Neuroscience & Mental Health animal ethics committee. All mice were housed on a 12 hour light/dark cycle with ad libitum access to food and water. Adult female C57BL/6 mice were used as graft recipients while donor tissue for transplantation was obtained from time-mated mice expressing green fluorescent protein (GFP) under the β-actin promoter. Animals were time mated overnight and visualization of a vaginal plug on the following morning was taken as embryonic day (E) 0.5. Embryos at E14.5 were collected in chilled L15 media. GFP+ embryos were selected, their brains removed and the cortices dissected to isolate GFP+ cortical primary tissue. The cortices were incubated for 20 minutes in 0.1% DNase and 0.05% trypsin in magnesium and calcium HBSS. The tissue was then washed gently 3 times with HBSS. The tissue was then dissociated and the cells re-suspended in HBSS with 0.1% DNAse at 200 000 cells/μL.

Implantation of self-assembling peptide hydrogels with cell transplantation. Mice received implants of cells in the presence or absence of Fmoc-SAPs (Fmoc-DIKVAV; Fmoc-FRGDF; Fmoc-DYIGSRF), n = 6 per group. Mice were anaesthetized with 5% isoflurane, and the level of anesthesia maintained at 2% for the duration of the surgery. Mice were placed in a stereotaxic frame, midline incisions were made in the scalp and craniotomies were performed overlying the striatum. Cells were mixed at a 1:1 ratio with HBSS or Fmoc-SAP prior to implantation into the striatum. A total of 2 μl (200,000 cells) were injected, using a fine glass capillary, at the following co-ordinates: 1.0 mm anterior and 2.5 mm lateral relative to bregma, and at a depth of 3.2 mm below the dural surface. After 28 days, mice were delivered a terminal dose of barbiturate and were transcardially perfused with warm saline followed by 4% paraformaldehyde (PFA). Brains were removed and post-fixed for 2 hours in 4% PFA before overnight cryo-preservation in 30% sucrose solution. The brains were then coronally sectioned at 40 μM in 12 series before free-floating immunohistochemistry was performed.

Immunohistochemistry. Free floating immunohistochemical procedures were performed as previously described.[26] Primary antibodies and dilution factors were as follows: chicken anti-GFP (GFP, 1:1000, Abcam), rabbit anti-GFAP (GFAP, 1:800, DAKO) and mouse anti-CD11b (1:100, AbD serotec). Secondary antibodies for direct detection were used at a dilution of 1:200 — DyLight 488 conjugated donkey anti-chicken, DyLight 550 donkey anti-rabbit and DyLight 649 donkey anti-mouse (Jackson ImmunoResearch). Absolute cell counts and optical density measurements were carried out on a Leica fluorescent microscope (Leica CTR6000).

Assessment of grafts. Grafted cells, and the extent of their innervation were discernable by the presence of GFP+ staining. For all animals, total number of GFP+ cell, density (GFP+ cells/mm^3) and volume of innervation (mm^3) were quantified. Optical intensity was measured at two fields of view (FOV) for comparison of innervation between each group. This technique was also used for assessment of inflammation. ImageJ was used to determine the optical intensity of the fluorophore (488 for GFP; 550 for GFAP and 649 for CD11b) in each image at each FOV. This provides a relative comparison for the extent of innervation or elicited inflammatory response induced in each group.

Statistical analysis. One-way ANOVAs with Tukey post-hoc tests were used to identify statistically significant changes between groups. The data was also transformed in order to obtain equal variance and the tests repeated, however, this had no effect on the statistical information obtained. Statistical significance was set at a level of $P < 0.05$. Data represents mean ± standard error of the mean (SEM).

Results and discussion

Laminin and fibronectin based Fmoc-SAPs form nanofibrous hydrogels at physiological pH

Three Fmoc-SAPs containing laminin and fibronectin peptide binding domains were designed and optimized for self-assembly under physiological conditions (pH 7.4) *via* two previously developed approaches.[12, 24] Fmoc-aspartate-isoleucine-lysine-valine-alanine-valine (Fmoc-DIKVAV) and Fmoc-aspartate-tyrosine-isoleucine-glycine-serine-arginine-phenylalanine (Fmoc-DYIGSRF) were designed via adjusting their pKa with an N-terminal acidic residue, namely aspartate **(Figure 1 A & B)**.[12] Alternatively,

uncharged flanking aromatic residues were added to improve the stability of the assembly to give Fmoc-phenylalanine-arginine-glycine-aspartate-phenylalanine (Fmoc-FRGDF) (**Figure 1 C**).[24]

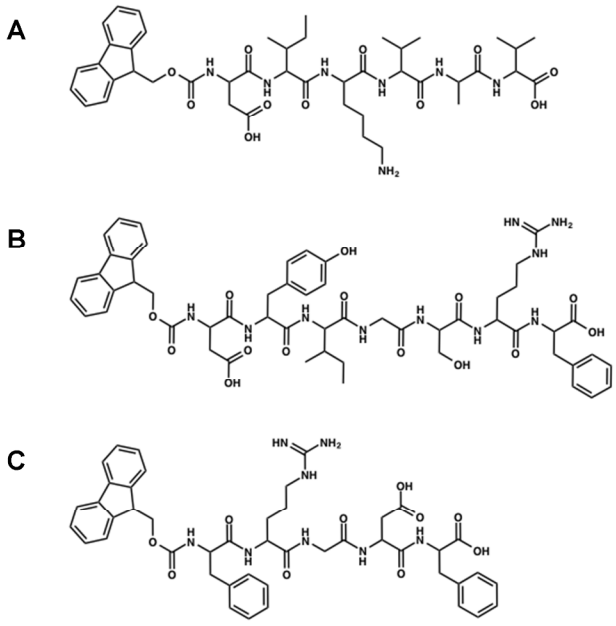

Figure 1. Chemical structure of (A) Fmoc-DIKVAV, (B) Fmoc-DYIGSRF and (C) Fmoc-FRGDF.

Fmoc-self-assembly occurs when individual peptide building blocks are optimally charged, undergoing π-π stacking between aromatic Fmoc groups and hydrogen bonding between the pendant peptide groups, to form individual nanofibers. The short peptide chains assemble in anti-parallel β-sheets, yielding an overall π-β assembly **(Figure 2)**.

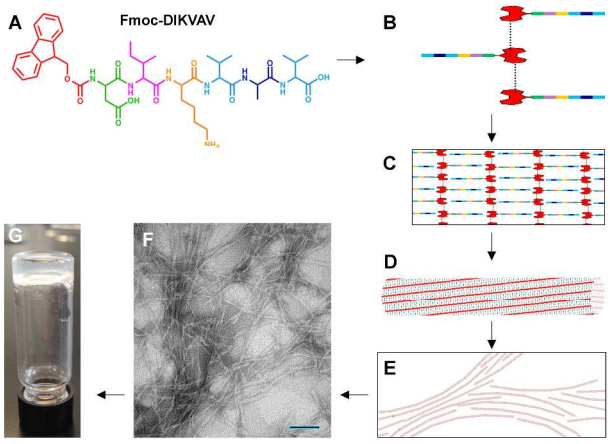

Figure 2. Schematic of Fmoc-self-assembly process with Fmoc-DIKVAV. (A) Fmoc-DIKVAV structure as synthesized via solid-phase peptide synthesis. (B) Aromatic Fmoc terminal groups undergo π-π stacking. (C) The DIKVAV peptide chains undergo hydrogen bonding to form anti-parallel β-sheets. (D) A natural twist occurs to maintain this π-β assembly forming a hollow nanofiber with the DIKVAV sequence exposed on the outside of the fiber. (E) The nanofibers interact with each other forming a nanofibrous network as shown in (F), TEM of resulting Fmoc-DIKVAV hydrogel (scale bar 100 nm). (G) The material presents as a shear-thinning hydrogel.

To ensure the underlying non-covalent and supramolecular interactions leading to π-β assembly were maintained with the insertion of bioactive peptide sequences, a series of materials characterization techniques were performed. AFM showed that each hydrogel presented a microscale fibrous network broadly analogous in scale, consisting of entwined linear features **(Figure 3 A - C)**. TEM micrographs showed that in each case, fibrils nanometers in diameter and microns in length were formed and these appeared to orientate laterally, forming entanglements **(Figure 3 D - F)**. Though the nanofibers were broadly conserved across all three systems, a more branched architecture was observed for Fmoc-DYIGSRF with fibers slightly larger in diameter than those seen for Fmoc-FRGDF and Fmoc-DIKVAV, potentially an effect of bundling fibers due to increased relative charge **(Figures 3 C & F)**. Though IKVAV and YIGSR are both laminin based peptides, the observed differences in structure is a direct result of their unique amino acid sequence, apparent pKa of the peptide, hydrophobicity of the sequence and resulting charge at physiological pH.[23]

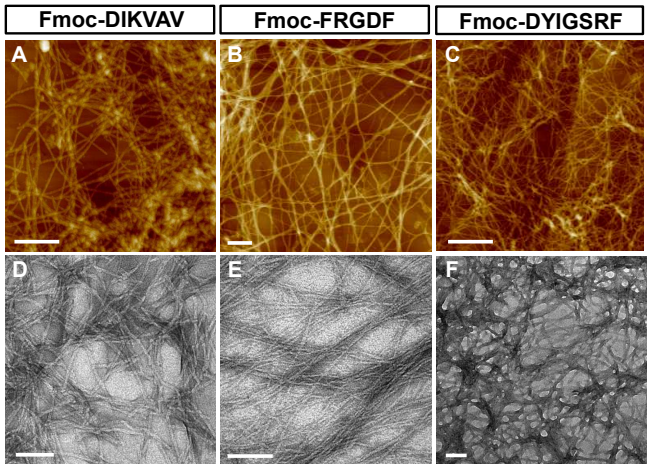

Figure 3. (A-C) AFM (scale bar 500 nm) and (D-F) TEM (scale bar 100 nm) showing nanofibrous architecture of the three Fmoc-SAPs: Fmoc-DIKVAV, Fmoc-FRGDF and Fmoc-DYIGSRF.

In order to determine the viscoelastic properties of the hydrogels, parallel plate rheology was performed. The materials displayed characteristic viscoelastic gel properties, namely a storage modulus (G') greater than the loss modulus (G") with both moduli independent of frequency **(Figure 4 A - C)**.[17] The moduli varied across the three different sequences, attributed to the varying charges that appear throughout each unique sequence and the resulting ionic interactions between the individual fibrils. At the same concentration, Fmoc-DIKVAV showed the strongest rheological properties with a G' of 30 000 Pa **(Figure 4 A)**. Fmoc-FRGDF and Fmoc-DYIGSRF were significantly weaker with a G' of ~100 Pa and ~200 Pa respectively, which could be a result of the morphological differences observed **(Figure 4 B & C)**. Importantly, the range of moduli present is comparable to a range of soft tissues and could therefore be tuned for tissue specific applications.

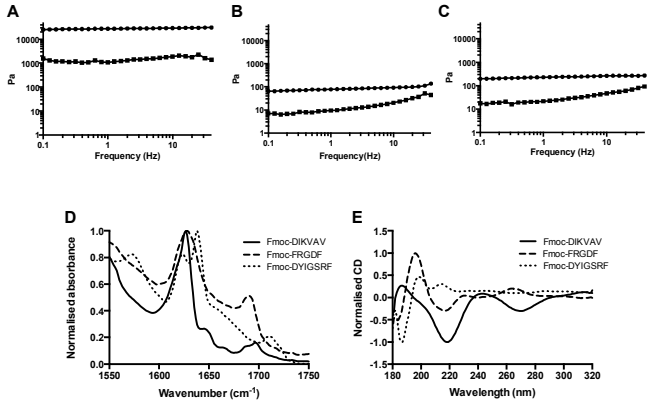

Figure 4. Rheological analysis showing characteristic viscoelastic behavior, where G' (circles) is greater than G" (squares) for (A) Fmoc-DIKVAV, (B) Fmoc-FRGDF and (C) Fmoc-DYIGSRF. (D) FTIR analysis of amide I region showing characteristic peaks for antiparallel β-sheets. (E) CD shows transition peaks at 220 nm for all the synthesized Fmoc-SAPs, suggesting the presence of β-sheets. Transitions in the 230 – 270 nm region represent supramolecular ordering and bundling of individual fibers.

Spectroscopic analyses of the Fmoc-SAP hydrogels were used to confirm that across each sequence the underlying π-β assembly was conserved. FTIR was used to investigate the presence of secondary structure by monitoring intermolecular 'peptide-like' interactions across the amide I region **(Figure 4 D)**.[17] In each case, vibrations characteristic of this class of SAPs were observed. Anti-parallel β-sheet formation were observed with a major peak between 1630 – 1660 cm^{-1} and a minor peak between 1690 - 1710 cm^{-1}.[17, 21] In addition, a broad feature at ~1650 cm^{-1} was observed, indicative of a random coil component.[21] Intra- and supramolecular interactions were analysed using CD **(Figure 4 E)**. A general n-π* transition between 180 and 220 nm was observed in each sample, indicating the formation of anti-parallel β-sheets **(Figure 4 E)**.[27] Transitions in the range of 230 – 270 nm arise due to the supramolecular alignment of individual fibers and are characteristic of Fmoc-SAPs.[28] Again, the CD spectrum for Fmoc-DYIGSRF indicates the presence of some random coil structures. However, together with the TEM and AFM images, the spectroscopic analysis confirms that π-β self-assembly is a robust mechanism that allows the formation of nanofibrous structures, despite the incorporation of varying bioactive peptide sequences, extending the peptide sequence, and altering the hydrophobicity and charge of the peptide sequence.

Response of cortical neural progenitor cells upon transplantation into the mouse brain using Fmoc-SAPs

Fmoc-SAPs support the survival and migration of transplanted cortical neural progenitor cells in the intact brain. Following characterization of the Fmoc-SAPs, their capacity to support cell grafts *in vivo* was assessed in the intact brain. E14.5 cortical neural progenitor cells expressing GFP were stereotaxically injected into mouse brains (the striatum) in the absence or presence of Fmoc-SAPs. The grafted cells were identified by GFP staining within the mouse brain.

A GFP+ cell count showed no statistically significant difference in survival between cells alone and cells implanted together with Fmoc-SAPs, demonstrating that in each case the Fmoc-SAPs were non-cytotoxic **(Figure 5 A)**. Not surprisingly, there was a trend for grafts in the presence of Fmoc-FRGDF to have the lowest GFP+ cell survival rate compared to Fmoc-DIKVAV and Fmoc-DYIGSRF **(Figure 5 A)**. This is supported by the known role of laminin, but not fibronectin, as a major constituent of the brain's ECM and modulator of neural differentiation and neurite extension.[29] This emphasizes the importance of designing a microenvironment that is specifically tuned to cellular requirements for tissue specificity. The density of cells within the graft core was assessed as an index of cell migration (GFP+ cells/mm^3, **Figure 5 A**). Similar to cell survival, graft cell density showed no significant difference between any groups **(Figure 5 A)**.

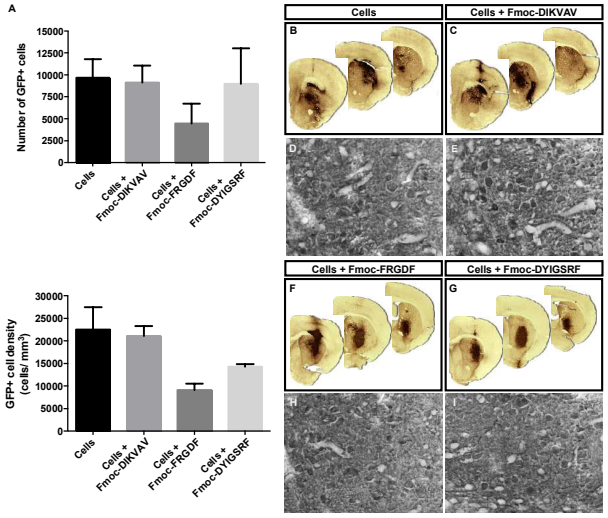

Figure 5. (A) Number of GFP+ cells in the striatum 28 days after transplantation (top) and cell density of implanted GFP+ cells in graft core (bottom). Data represents mean + SEM. Photomontages of the mouse brain illustrating GFP+ grafts in (B) the absence, and presence of (C) Fmoc-DIKVAV, (F) Fmoc-FRGDF and (G) Fmoc-DYIGSRF. (D, E, H & I) show high power magnification (10 x) of GFP+ grafts.

With no statistical difference observed in cell survival or migration between grafts in the presence or absence of Fmoc-SAP, we have shown that these scaffolds are non-cytotoxic to grafted cells in the parenchyma. This result demonstrates the capacity for these non-toxic materials to support cells, potentially in a disease setting. The Fmoc-SAPs could help rebuild tissue by supporting the surrounding parenchyma, enhancing the graft-host interface at the lesion site to reduce any potential for secondary degeneration whilst also encouraging integration of transplanted cells with the host tissue.

Grafted cortical neural progenitor cells can innervate the host brain tissue in the presence of Fmoc-SAPs. Integration of transplanted cells within the host environment and reinnervation of damaged host tissue by transplanted cells have been identified as key issues in clinical trials for cell replacement therapy and are important goals in order to achieve lasting recovery and repair of neural circuitry.[31] Here, the volume of GFP+ graft innervation was determined in animals grafted with cells in the absence or presence of Fmoc-SAPs. No statistical difference in the level of innervation was observed between groups **(Figure 6 A)**. Similar to cell survival, cells in the presence of Fmoc-FRGDF demonstrated the least capacity for innervation of the host brain, with the smallest volume of innervation **(Figure 6 A)**.

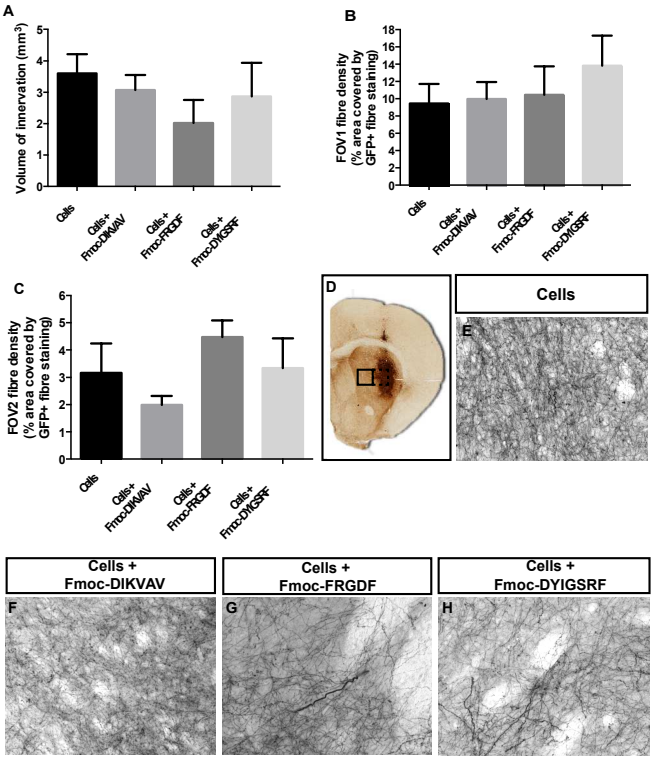

Figure 6. (A) Volume of GFP+ graft innervation. (B & C) Percentage of GFP+ fibers in FOV1 and FOV2 respectively for each group, measured as optical density. (D) Section of single brain hemisphere showing example of fields of view (FOV) 1 (dashed line box) and 2 (solid line box) taken from the edge of the graft core, sequentially moving outwards. (E – J) Images of FOV2 used to measure optical density of GFP+ fibers and show fiber innervation. Data represents mean + SEM.

Additionally, we assessed the density of GFP+ graft fiber innervation at two pre-determined fields of view (FOV1 and FOV2) away from the edge of the graft core **(Figure 6 B - D)**. No significant difference was observed between the four groups, suggesting that the amount of neurite growth was not impeded by the Fmoc-SAPs **(Figures 6 B & C)**. Together, this data confirms that implanted cells are capable of extending neurites into the surrounding parenchyma, unhindered by the presence of Fmoc-SAPs, highlighting their capacity as a useful tool for the delivery of cells in cell transplantation therapy.

Implantation of Fmoc-SAPs into the intact mouse brain does not result in glial scarring. A key concern impeding neural plasticity following CNS injury is the formation of the glial scar. The glial scar is comprised of reactive astrocytes and microglia that help form a fibrotic scar to seal off the injury, but also secrete inhibitory proteins that prevent axon regeneration.[32-34] To further assess the biocompatibility of Fmoc-SAPs in the brain, the inflammatory microglial and astrocytic response to the materials was investigated.

Fmoc-DIKVAV and Fmoc-DYIGSRF showed no increase in host-derived (GFP-) astrocytes (glial fibrillary acidic protein; GFAP+) compared to cells transplanted alone **(Figure 7 A)**. Additionally, Fmoc-DIKVAV showed no increase in microglia (CD11b+) after 28 days **(Figure 7 B)**. These results suggest that the host environment does not recognize these Fmoc-SAPs as "foreign material", with a limited immune response elicited over the course of 28 days **(Figures 7 C – R)**. This is significant as these results emphasize the biocompatibility of these materials compared to other hydrogels, such as chitosan, that has been shown to be phagocytized by macrophages after 7 days *in vivo* due to the elicited foreign body response.[35]

After 28 days, Fmoc-FRGDF showed a trend towards enhanced astrocyte density compared to all other groups **(Figure 7 A)**. In addition, Fmoc-FRGDF showed a statistically significant increase in microglia recruitment ($P < 0.05$) compared to cells alone and the laminin based Fmoc-SAP, Fmoc-DIKVAV ($P < 0.0001$) **(Figure 7 B)**. Again, the control RGD sequence demonstrated the least biocompatibility for this application, however, as validated by the high GFP+ cell counts, the material itself is not cytotoxic **(Figure 5 A)**. Rather, as previously suggested, the RGD signal is not suitable for presentation to cells in the CNS.

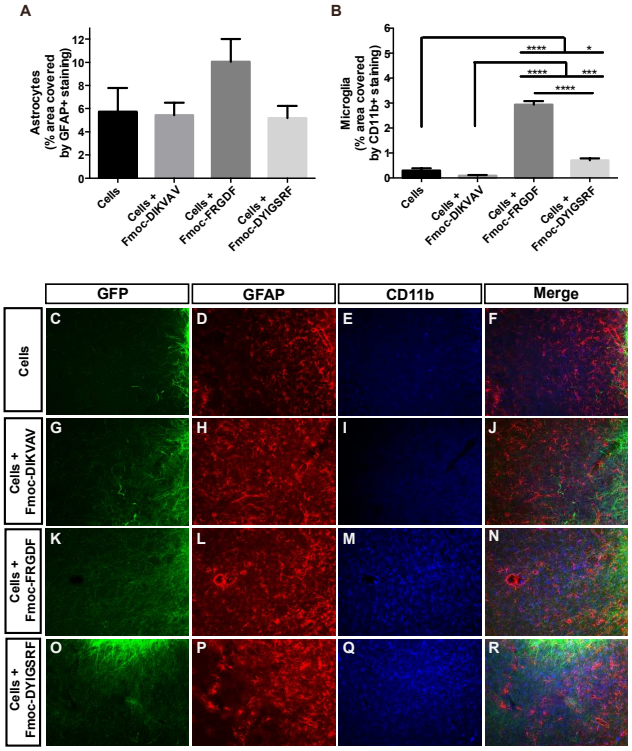

Figure 7. Inflammatory response to cells transplanted alone and with Fmoc-SAPs measured as percentage of coverage of FOV at edge of graft (fluorescent optical density) (A) Astrocytic response, (B) Microglial response, (C – R) Images of transplanted neural progenitor cells (GFP+; green), astrocytes (GFAP; red) and microglia (CD11b; blue). Data represents mean + SEM. *$P < 0.05$, *** and ****$P < 0.0001$.

Previous studies have shown that Fmoc-peptides display neuroprotective properties where Fmoc-L-leucine protected both the mature and immature brain through the activation of PPARγ.[36] In addition, Fmoc-amino acids have been reported to have anti-inflammatory properties, inhibiting the recruitment of T-lymphocytes and neutrophils during an inflammatory response.[37] In line with these findings, here we demonstrated that after 28 days *in vivo* there was no glial scarring in the presence of any of the Fmoc-SAPs, indicating the inherent biocompatibility of these materials in the brain and their capacity to attenuate the inflammatory response. Importantly, this is the first study where Fmoc-SAPs have been used as a vehicle for the delivery and support of cell transplants *in vivo*. Their observed biocompatibility and lack of induced immune

response promotes their suitability as a tool for cell transplantation in the brain.

Conclusion

Current research on Fmoc-SAPs has focused on understanding the material properties and underlying mechanisms of self-assembly of this system with their potential for biological applications being limited to small *in vitro* proliferation assays on cell lines. Here, we have demonstrated the utility of minimalist Fmoc-SAPs as biocompatible materials to support cell transplantation *in vivo*. We have developed three Fmoc-SAPs, containing varying ECM protein based peptides, for use as a delivery vehicle for neural progenitor cells for implantation into the intact mouse brain. The ability of the Fmoc-SAPs to maintain transplanted cell survival and the lack of induced immune response suggests their potential suitability for supporting residual host cells surrounding an injury site, as well as integration of newly transplanted cells. These results give us confidence that incorporating short amino acid sequences into Fmoc-SAPs allows the design of materials that can be easily and specifically tuned to a particular tissue and/or cellular requirement and demonstrates that Fmoc-SAPs could be used as a platform for the design of enhanced microenvironments to promote tissue repair.

Acknowledgements

The acknowledgements come at the end of an article after the We would like to thank Dr Navdeep Kaur and Joanne Lee (Centre for Advanced Microscopy, ANU) for their help and guidance in preparing negative stains for TEM imaging and Francesca Maclean and Shayanti Mukerhjee for thorough proof reading of the manuscript. This research was supported by funding from the National Health and Medical Research Council (NHMRC), Australia and the Australian Research Council. ALR was supported by an Australian Postgraduate Award; CLP was supported by an NHMRC Career Development Award, and subsequently Senior Medical Research Fellowship provided by the Viertel charitable Foundation, Australia; DRN was supported by an Australian Research Council Australian Postdoctoral Fellowship, and subsequently by a NHMRC Career Development Fellowship; and RJW is funded via an Alfred Deakin Research Fellowship. The Florey Institute of Neuroscience and Mental Health acknowledges the support from the Victorian Government's Operational Infrastructure Support Grant.

Notes and references

[a] Research School of Engineering, The Australian National University, Canberra, Australia, 0200.
[b] Florey Institute of Neuroscience & Mental Health, The University of Melbourne, Parkville, Australia, 3010.
[c] Centre for Chemistry and Biotechnology, Deakin University, Waurn Ponds, Australia, 3217.
[d] School of Aerospace, Mechanical and Manufacturing Engineering, RMIT University, Melbourne, Australia, 3001.
* Both authors contributed equally to this work.

Electronic Supplementary Information (ESI) available: [details of any supplementary information available should be included here]. See DOI: 10.1039/b000000x/

1. A. Bjorklund, *Novartis Found Symp*, 2000, **231**, 7-15; discussion 16-20.
2. C. L. Parish and L. H. Thompson, *Journal of molecular cell biology*, 2014, **6**, 54-63.
3. O. Lindvall and Z. Kokaia, *The Journal of clinical investigation*, 2010, **120**, 29-40.
4. S. B. Dunnett and A. E. Rosser, *Neurobiology of disease*, 2014, **61**, 79-89.
5. O. Lindvall and Z. Kokaia, *Stroke*, 2011, **42**, 2369-2375.
6. J. T. S. Pettikiriarachchi, C. L. Parish, M. S. Shoichet, J. S. Forsythe and D. R. Nisbet, *Australian Journal of Chemistry*, 2010, **63**, 1143-1154.
7. D. R. Nisbet, J. A. Bourne and J. S. Forsythe, in *Biomaterials Developments and Applications*, eds. H. Bourg and A. Lisle, NOVA Publishers, 2010, pp. 453-463.
8. D. R. Nisbet, A. E. Rodda, M. K. Horne, J. S. Forsythe and D. I. Finkelstein, *Biomaterials*, 2009, **30**, 4573-4580.
9. T. Y. Wang, J. S. Forsythe, D. R. Nisbet and C. L. Parish, *Biomaterials*, 2012.
10. R. Timpl and J. C. Brown, *BioEssays*, 1996, **18**, 123-132.
11. D. R. Nisbet and R. J. Williams, *Biointerphases*, 2012, **7**, 2.
12. A. L. Rodriguez, C. L. Parish, D. R. Nisbet and R. J. Williams, *Soft Matter*, 2013, **9**, 3915-3919.
13. V. M. Tysseling-Mattiace, V. Sahni, K. L. Niece, D. Birch, C. Czeisler, M. G. Fehlings, S. I. Stupp and J. A. Kessler, *Journal of Neuroscience*, 2008, **28**, 3814.
14. T. C. Holmes, S. de Lacalle, X. Su, G. Liu, A. Rich and S. Zhang, *Proceedings of the National Academy of Sciences*, 2000, **97**, 6728-6733.
15. R. Orbach, L. Adler-Abramovich, S. Zigerson, I. Mironi-Harpaz, D. Seliktar and E. Gazit, *Biomacromolecules*, 2009, **10**, 2646-2651.
16. R. Williams, A. Smith, R. Collins, N. Hodson, A. Das and R. Ulijn, *Nature Nanotechnology*, 2008, **4**, 19-24.
17. A. Smith, R. Williams, C. Tang, P. Coppo, R. Collins, M. Turner, A. Saiani and R. Ulijn, *Advanced materials*, 2008, **20**, 37-41.
18. H. Xu, A. K. Das, M. Horie, M. S. Shaik, A. M. Smith, Y. Luo, X. Lu, R. Collins, S. Y. Liem, A. Song, P. L. A. Popelier, M. L. Turner, P. Xiao, I. A. Kinloch and R. V. Ulijn, *Nanoscale*, 2010, **2**, 960-966.
19. C. Tang, A. Smith, R. Collins, R. Ulijn and A. Saiani, *Langmuir*, 2009, **25**, 9447-9453.
20. M. Zhou, A. Smith, A. Das, N. Hodson, R. Collins, R. V. Ulijn and J. Gough, *Biomaterials*, 2009, **30**, 2523-2530.
21. G. Cheng, V. Castelletto, R. R. Jones, C. J. Connon and I. W. Hamley, *Soft Matter*, 2011, **7**, 132601333.
22. V. Jayawarna, S. M. Richardson, A. R. Hirst, N. W. Hodson, A. Saiani, J. E. Gough and R. V. Ulijn, *Acta Biomater*, 2009, **5**, 934-943.
23. D. J. Adams, L. M. Mullen, M. Berta, L. Chen and W. J. Frith, *Soft Matter*, 2010, **6**, 1971-1980.
24. V. N. Modepalli, A. L. Rodriguez, R. Li, S. Pavuluri, K. R. Nicholas, C. J. Barrow, D. R. Nisbet and R. J. Williams, *Peptide Science*, 2014.
25. L. F. Reichardt and K. J. Tomaselli, *Annual review of neuroscience*, 1991, **14**, 531.
26. C. R. Bye, L. H. Thompson and C. L. Parish, *Experimental neurology*, 2012, **236**, 58-68.
27. S. M. Kelly, T. J. Jess and N. C. Price, *Biochimica et Biophysica Acta (BBA)-Proteins and Proteomics*, 2005, **1751**, 119-139.

28. A. R. Hirst, S. Roy, M. Arora, A. K. Das, N. Hodson, P. Murray, S. Marshall, N. Javid, J. Sefcik and J. Boekhoven, *Nature chemistry*, 2010, **2**, 1089-1094.
29. V. Tysseling, V. Sahni, E. Pashuck, D. Birch, A. Hebert, C. Czeisler, S. Stupp and J. Kessler, *Journal of neuroscience research*, 2010, **88**, 3161-3170.
30. D. M. Ryan and B. L. Nilsson, *Polymer Chemistry*, 2012, **3**, 18-33.
31. C. Winkler, D. Kirik and A. Björklund, *Trends in neurosciences*, 2005, **28**, 86-92.
32. A. Rolls, R. Shechter and M. Schwartz, *Nature Reviews Neuroscience*, 2009, **10**, 235-241.
33. C. L. Lau, M. Kovacevic, T. S. Tingleff, J. S. Forsythe, H. S. Cate, D. Merlo, C. Cederfur, F. L. Maclean, C. L. Parish and M. K. Horne, *Journal of Neurochemistry*, 2014.
34. J. E. Burda and M. V. Sofroniew, *Neuron*, 2014, **81**, 229-248.
35. K. Crompton, D. Tomas, D. Finkelstein, M. Marr, J. Forsythe and M. Horne, *Journal of Materials Science: Materials in Medicine*, 2006, **17**, 633-639.
36. P. Maurois, S. Rocchi, N. Pages, P. Bac, J. P. Staples, P. Gressens and J. Vamecq, *Biomedicine and Pharmacotherapy*, 2008, **62**, 259-263.
37. R. M. Burch, M. Weitzberg, N. Blok, R. Muhlhauser, D. Martin, S. G. Farmer, J. M. Bator, J. R. Connor, C. Ko, W. Kuhn, B. A. McMillan, M. Raynore, B. G. Shearer, C. Tiffany and D. E. Wilkins, *Proceedings of the National Academy of Sciences of the United States of America*, 1991, **88**, 355-359.

Functionalized N-fluorenylmethyloxycarbonyl self-assembling peptides are biocompatible *in vivo*, demonstrating their utility as a cell delivery vehicle for tissue engineering.